Volume 14 | Number 12 | 21 June 2014 | Pages 1953–2132

Lab on a Chip

Miniaturisation for chemistry, physics, biology, materials science and bioengineering

www.rsc.org/loc

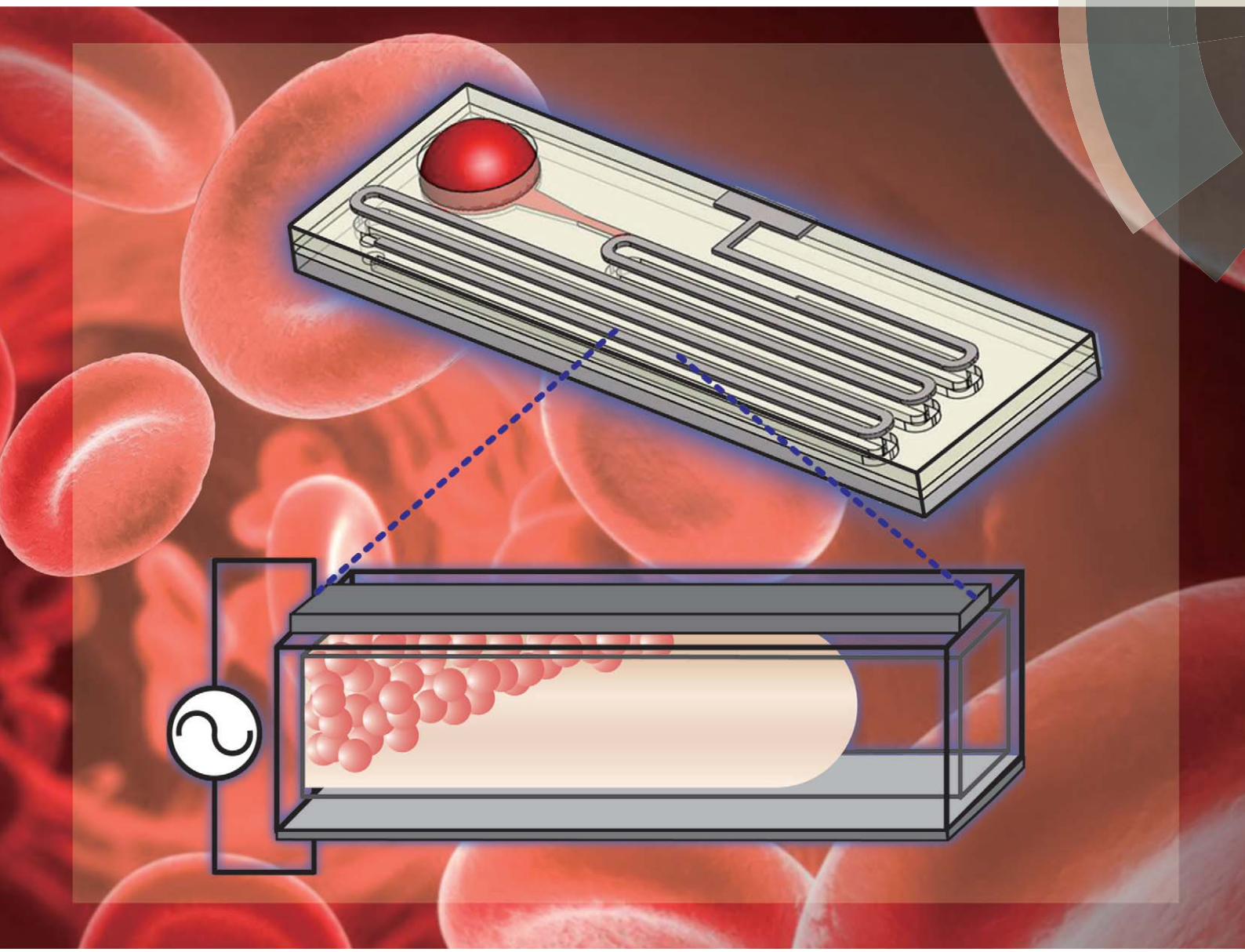

ISSN 1473-0197

ROYAL SOCIETY OF CHEMISTRY

PAPER

Chen-Kuei Chung *et al.*

Microfluidic chip for plasma separation from undiluted human whole blood samples using low voltage contactless dielectrophoresis and capillary force

Lab on a Chip

PAPER

Microfluidic chip for plasma separation from undiluted human whole blood samples using low voltage contactless dielectrophoresis and capillary force†

Cite this: *Lab Chip*, 2014, **14**, 1996

Chia-Chern Chen,[a] Po-Hsiu Lin[b] and Chen-Kuei Chung*[b]

Received 13th February 2014,
Accepted 18th March 2014

DOI: 10.1039/c4lc00196f

www.rsc.org/loc

A plasma separating biochip is demonstrated using a capillary-driven contactless dielectrophoresis method with low voltage (~1 V) and high frequency induced electrostatics between red blood cells. The polarized red blood cells were aggregated and separated from plasma with a 69.8% volume separation and an 89.4% removal rate of red blood cells.

Introduction

Many microfluidic devices for plasma separation from whole blood samples have already been developed. Most methods used centrifugal force,[1,2] and the red blood cells, white blood cells, and platelets were captured using microfilters.[3,4] Changing the geometry of a microchannel allows different forces to be created in the channel for separation. For example, separation could occur by using inertial force[5,6] and the Zweifach–Fung effect, which is a phenomenon where particles at the branching points of microchannels tend to flow into the wider channel, which has a faster flow rate.[7,8] However, these devices required external mechanical driving sources such as a syringe pump, and tube connections between the devices and their mechanical driving sources. Dielectrophoresis (DEP) is one of the well-established techniques used to produce a deterministic force for the manipulation of microscale and nanoscale particles. The DEP technique allows plasma separation and blood cell sorting using an electrical force caused by an inhomogeneous electric field between two electrodes.[9–11] Yet, this technique required diluted blood samples, contact between the samples and the electrodes, and the applied voltages were high, mostly over 100 V.[12,13] This could damage the red blood cells and hemoglobin released from the ruptured red blood cells (RBCs) could pollute the separated plasma. The high voltage applied may cause electrochemical effects, bubble formation, and the detrimental effect of joule heating in the sample.[14,15] The absence of contact between electrodes and samples prevents bubble formation, and decreases heat production. Contamination of electrodes can also be avoided.[16,17]

Here we developed a portable, disposable, capillary-driven and low-voltage (~1 V) contactless dielectrophoresis (cDEP) microfluidic chip for the separation of plasma from undiluted whole blood. The electrodes are capacitively-coupled to the microfluidic channel with an inhomogeneous high-frequency electric field applied to induce an electrostatic force between the cells in the channel. The cDEP effect for the polarized and aggregated cells, together with the capillary force, produced a velocity difference between the red blood cells and the plasma resulting in separation of the two components. The volume separation efficiency was more than 69.8% and the separation quality (removal rate of RBCs) was 89.4%. The separated plasma showed that the residual RBCs were not damaged by the electric field and no hemolysis was detected.

Theory and measurements

In an alternating current (AC) electric field, the time-averaged DEP force, F_{dep}, assumes that the particle is isolated and that the dipole limit is valid.[18] When the particle is more polarizable than the medium, the particle will be attracted towards the strong electric field (positive DEP). When the particle is less polarizable than the medium, it will be repelled away from the strong electric field (negative DEP).

In the undiluted sample case, electrical permittivity of the suspension becomes dependent on the particle volume fraction. Therefore, concentration dependent Maxwell–Wagner expressions, in quasi-steady-state electrodynamic conditions, should be employed to obtain the DEP force.[19,20] In this study, positive DEP drove the red blood cells towards the stronger electric field, the upper electrode surface of the chip.

[a] *Department of Family Medicine, St Martin de Porres Hospital, Chiayi City, Taiwan, Republic of China*
[b] *Department of Mechanical Engineering, National Cheng Kung University, Taiwan, Republic of China. E-mail: ckchung@mail.ncku.edu.tw; Fax: +06 2352973; Tel: +06 2757575 62111*

† Electronic supplementary information (ESI) available. See DOI: 10.1039/c4lc00196f

The whole blood sample was driven along the channel by capillary force, which is based on the contact angle, the geometry of the channel and the surface tension. Though the pressure difference remained the same, the drive will decrease gradually due to the increasing mass of the whole blood or plasma sample running from the inlet into the channel over time, as shown in the results and discussion section.

Whole blood (3.5 mL) was sampled from a healthy adult volunteer through venipuncture. The sampled blood was mixed with 3.8% buffered sodium citrate in a test tube to prevent coagulation. The performance of the device was checked using 150 μL whole blood samples. A signal function generator applied the AC voltage to the chip. The behavior of the blood cells and plasma were monitored by an optical microscope and checked through visual inspection.

To determine that the function of the chip worked with the contactless dielectrophoresis, the separation efficiency of plasma (percentage of plasma (volume) harvested) and separation quality (removal rate of the RBCs) were developed. The separation efficiency of plasma was estimated and defined as:

$$\text{plasma (volume) harvested} = \frac{\frac{L_p}{L_p + L_c} \times 100\%}{100\% - \text{Hct}} \times 100\% \quad (1)$$

Where L_p and L_c are the lengths of the channel occupied by the plasma and red blood cells in the chip, respectively. It is supposed that the geometry is uniform throughout the entire channel. Hct is the hematocrit of the whole blood sample, which was detected in the lab by conventional methods. The measurement of both the occupied lengths of plasma and cells was carried out after stopping the flow of both the plasma and cell components in the channel. Additionally, the whole blood light absorbance of hemoglobin in the whole blood sample was related to the concentration of the hemoglobin carried by RBCs in the blood, which obeyed Beer's law.[21] In optics this indicates that the light absorbance is relative to the concentration of the solution. The bigger the light absorbance, the higher the concentration of solute in the solution. In this work, the separation quality (removal rate of RBCs) was calculated by the original and modified Beer's laws using the light absorbance of hemoglobin of the whole blood sample, and was defined as:

$$\text{Beer's Law: } \log\frac{I_0}{I} = \log\frac{1}{T} = kc = A \quad (2)$$

where I_0 is the intensity of the incident light, I is the intensity of penetrated light, k is the absorption coefficient, which is assumed constant through all of the experiments, and T is the light percentage transmittance. In these experiments, all of the light percentage transmittances were detected using a micro spectrometer system (SD1200-LS-HA, OTO Photonics Inc., Taiwan) in the visible light wavelength range from 400 nm to 800 nm, and it was averaged as 8.4% and 76.9% for the whole blood and separated plasma, respectively. c is the concentration of hemoglobin of the separated plasma, which is approximately proportional to the absorption of light, A.

Then the separation quality is defined as:

$$\text{Separation quality} = \frac{H_b - c}{H_b} \times 100\% \quad (3)$$

Where H_b is the hemoglobin concentration in whole blood detected using the conventional method which, in this experiment, was 14.2 g dL^{-1}.

Design and fabrication of the device

The microfluidic chip was designed with two glass slides (7.5 cm (length) × 3.5 cm (width) × 1 mm (thickness), FEA company, Taiwan) for the cover and bottom substrates. The cover substrate was designed with tandem inlet and outlet holes drilled by a CO_2 laser: one hole is for the blood inlet and the other is for the air-hole. The Optically Clear Adhesive (OCA film, thickness 175 μm, type 8187, 3M Company, U.S.A) was first attached on the bottom substrate and then processed as a microchannel of 800 μm in width by CO_2 laser ablation and bonded with the drilled cover substrate. The diameters of the blood inlet and outlet holes were 11 mm and 2 mm. The average depth of the channels was about 175 μm.

Fig. 1 shows the schematic fabrication process of the microfluidic chip with channels, holes and electrodes using two glass slides and an OCA 8187 film. First, the cover glass was selectively ablated and drilled to form the holes, and the patterned polyimide film for metal electrode was formed using water-assisted CO_2 laser ablation,[22,23] sputtering coating and lift-off processes, respectively (Fig. 1(a)–(c)). Because glass is highly sensitive to thermal and mechanical stresses, water-assisted laser ablation was used to avoid thermal cracks. Second, the flat bottom glass slide was wholly downside coated with the metal electrode by sputtering, and the upside was adhesive coated by an OCA 8187 film which was drilled to form the inlet and outlet channels (Fig. 1(d)) using the above laser ablation method. Laser machining merits easy and fast fabrication and no photo mask was needed. The average channel depth was about 175 μm using a laser power of 4 watts and a scanning speed of 114 mm s^{-1} for one pass. No cracks on the cover or bottom glass surface were found.

Results and discussion

Fig. 2 shows the basic principle of this cDEP plasma separation microfluidic chip. It is based on AC capacitively-coupled electrode induced inhomogeneous electrostatic fields, which polarized the cells in the microchannels. The increased dipole–dipole interactions between the cells produced

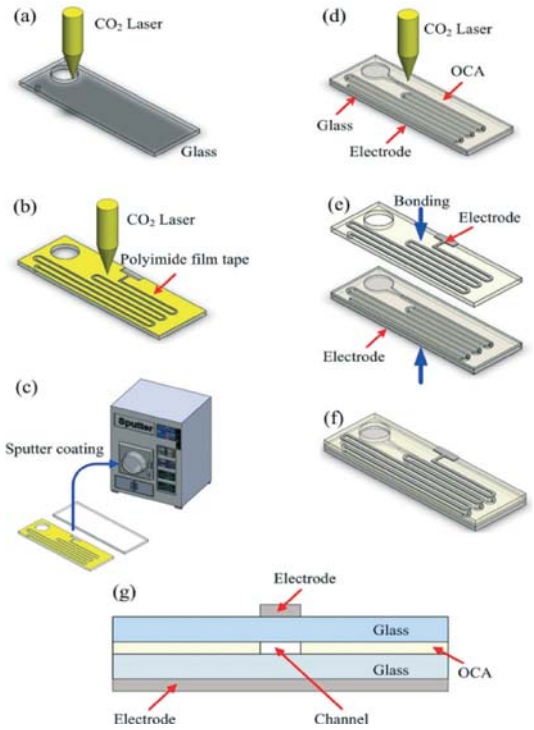

Fig. 1 (a–g) Schematic fabrication process used to create the microfluidic chip. (a) Water-assisted CO_2 laser ablation processing, (b) the pattern of the electrode ablated by CO_2 laser on a polyimide film tape, (c) metal sputtering, (d) the shape of the microchannel ablated by CO_2 laser on an OCA tape, (e) removing the film tape and bonding both chips together, (f) the fabricated integrated chip, and (g) a cross-section of the chip.

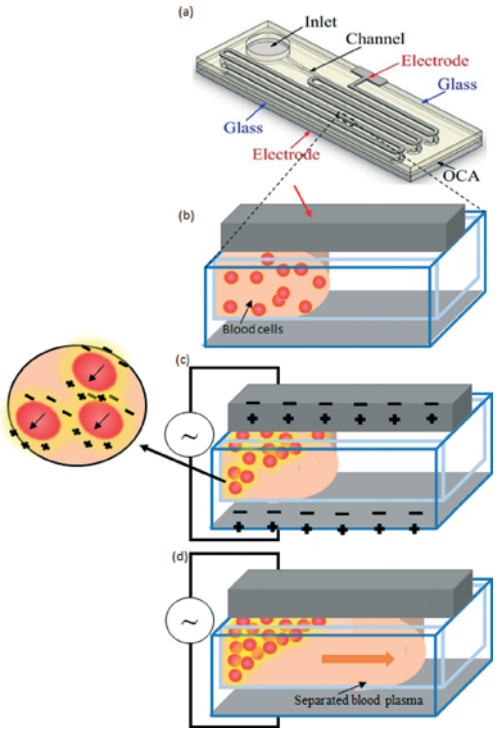

Fig. 2 The microfluidic plasma separation chip. (a) The schematic top and side views, (b) the red blood cells spread everywhere in the plasma during the voltage off stage, (c) the dipole–dipole interacting red blood cells after the voltage is turned on initially. The positive DEP force moves the red blood cells towards the top surface of the electrode. (d) The red blood cells aggregate to resist the capillary force and do not move, yet the plasma continues moving forwards after a long enough period of time.

velocity differences between the aggregated cells and the plasma, driven by capillary force. First, when introduced into the inlet of the chip, the human whole blood moved quickly due to the capillary force from the hydrophilic property of the glass, which was used to make both the top and bottom walls of the channel. At this point, the velocity of the red blood cells and plasma is the same (Fig. 2(b)).

When the AC voltage was applied, the inhomogeneous capacitively-coupled electric field was produced because of the geometrically asymmetric electrodes. The polarized red blood cells interacted with each other due to the electrostatic force and aggregated (Fig. 2(c)). Once the dipole–dipole interaction forces between cells were strong enough to counter the capillary force, the velocity of the aggregated cell mass slowed down. The velocity of the plasma was not affected by the electric field and continued to be driven quickly by the capillary force (Fig. 2(d)). The plasma was successfully separated from the whole blood sample as shown in the experimental result images in Fig. 3 (see more from the video in the ESI†).

The hematocrit is calculated by the ratio between the volume of RBCs and the total volume of blood sample, and indicates the rough ratio of RBCs in a sample. The same method is applied to calculate the percentage of plasma harvested. Due to the aggregation of red blood cells and the separation of plasma in the channel with a uniform shape, the hematocrit can be estimated using the same definition, with the volume substituted with the occupied length of each component. Therefore, the quality of the plasma harvested can be extensively defined into terms of separation efficiency (eqn (1)) and separation quality (removal rate of red blood cells, eqn (3)). Fig. 4 shows that the RBCs gradually disperse with time when the AC voltage is off in the stage of cell aggregation. After the AC voltage is off for 90 s, most of the RBCs and plasma have mixed together. It supports the theory (Fig. 2) of how our plasma separation chip functions.

Three experiments for each of five trials were carried out in order to evaluate blood separation times according to different frequencies and voltages. Each data point consists of at least three observations. The relationship between the frequency and the separation time under an AC voltage of 1 Vp-p are shown in Fig. 5, the correlation constant R^2 is 0.903. The peak-to-peak voltage, Vp-p, is the voltage difference between the maximum positive and the maximum negative amplitudes of a waveform. The separation time ranged from over 5000 seconds for the low frequency of 100 kHz to only 825 seconds for the high frequency of 10 MHz, as the voltage was applied immediately after the blood sample was sent into the channel. No plasma separation was observed under 100 kHz, and 1 Vp-p was applied until the whole blood sample reached

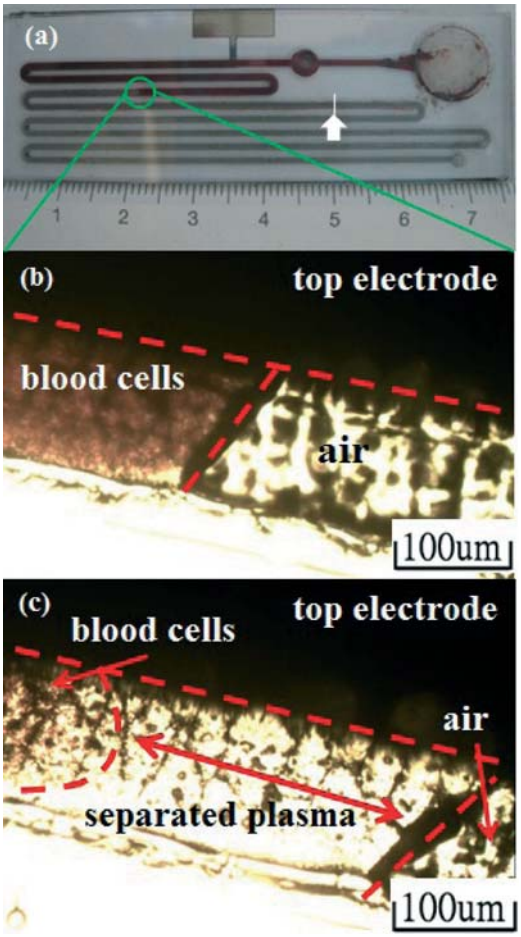

Fig. 3 Separation results for: (a) plasma separation shown from the backside of the chip, and the arrow indicates the location where the end of plasma is. (b) In the voltage off stage, the blood cells are still mixed with plasma and spread everywhere. Both had the same velocity and a near straight interface with air. (c) Voltage was on over a short period of time. The dipole–dipole attracted cells interacted aggressively with each other and aggregated, yet the plasma continued moving forward and separated with a meniscus interface between the cells and the plasma.

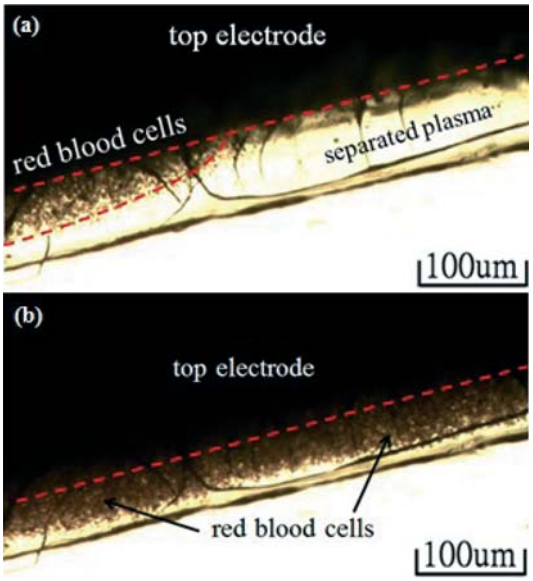

Fig. 4 The reaction of RBCs to an asymmetrical AC electric field: (a) voltage on, aggregation and (b) voltage off for 90 s, dispersal.

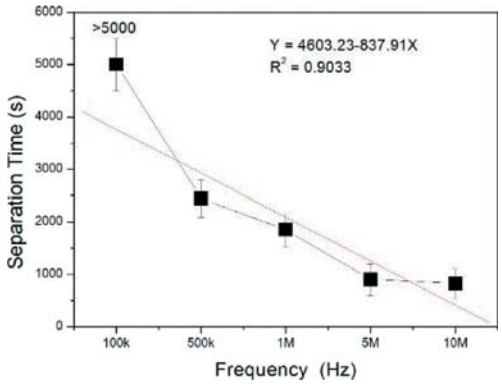

Fig. 5 The relationship between frequency and separation time under a constant voltage of 1.0 Vp-p, the correlation constant is 0.903. Each data point consists of at least three observations with one standard deviation as the error bar.

the outlet of the channel. Thus it is assumed that only a weak or minimal increase of particle dipole–dipole interactions occurs between the cells under 1 Vp-p and 100 kHz. Moreover, the low frequency AC electric field may be blocked off by the cell membranes, although there is sufficient retardation time for the cells to be polarized. In contrast, as the frequency increased, the separation time decreased, that is, the high frequency AC electric field induced more prominent dipole–dipole interactions between the cells. The separation time of the whole blood sample under a frequency of 100 kHz was more than 5000 s. No separation was noted even when the sample ran until the end of the channel. The applied voltage controls the magnitude of the electric field in the channel. The relationship between the applied voltage and separation time under the condition of 1 MHz constant frequency is shown in Fig. 6, and its correlation constant R^2 is 0.945. The separation time decreased with the applied

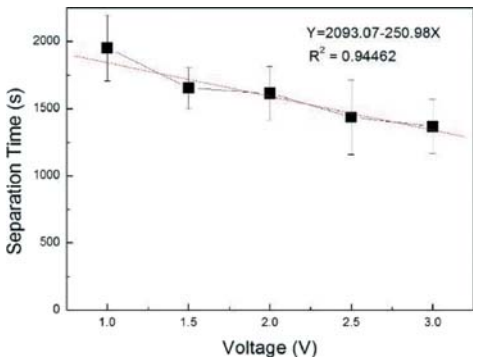

Fig. 6 The relationship between the applied voltage and separation time with the correlation constant value 0.945. Each data point consists of at least three observations with one standard deviation as the error bar.

voltage increasing from 1 Vp-p to 3 Vp-p, which demonstrated that besides frequency, increasing the voltage could enhance the interactions between cells too. Although the electric field was weak due to the thickness of both the top and the bottom substrate glasses, the cells aggregated and could separate from the plasma with capillary-driven flow. So, in order to increase the dipole–dipole interactions between cells, higher frequencies and voltages can be applied, which shortens the separation times. The conventional DEP methods used for particle separation with contact electrodes use high voltages, mostly over 100 V.[12,13] In comparison, the voltages required in this work were below 3 Vp-p. Even 1 Vp-p was enough for the separation of plasma from undiluted whole blood samples, as demonstrated in this chip. We noticed that for all of the voltages and frequencies investigated here, the RBCs moved towards the upper electrode along the channel, and therefore experienced positive dielectrophoresis.

Capillary driving force depends on the pressure differences between the inlet and the outlet, the material's properties, and the contact angles. As blood is a complex material, the capillary force may vary with cell and plasma distribution after cell aggregation. Also, the mass of the sample was increasing gradually in the channel due to the continuous inflow of the sample from the inlet. The increase of sample mass in the channel thus was time-dependent or distance-dependent, and decreased the blood flow velocity over time or distance. Under the influence of both the driven flow and the applied asymmetrical electric field, the blood flow velocity decreased as time passed (Fig. 7(a)). The varied flow velocity with distance influenced the separation times of plasma tested at 1 Vp-p and 1 MHz (Fig. 7(b)). Each data point consists of three observations with one standard deviation as the error bar. As the blood flow velocity decreased due to the increasing mass and material-dependent capillary force, shorter separation times were observed. Both the separation times and blood velocities decreased after increasing the time period before the applied voltage. In other words, the capillary driven force would keep driving the cells along the channel after the 1 MHz high frequency voltage was applied until the interaction force between the cells became strong enough to resist the driven force. It was noted that a separation time of over 1900 s for the high flow velocity sharply dropped to only 2 s for the low flow velocity. After enough dipole–dipole interactions between the cells were established, solid aggregation of the cells occurred. With the help of capillary driven force, plasma separation occurred effectively and quickly. Five trials were done for the separation efficiency determination work, and the average length of red blood cells (L_c) was 98.8 mm, and the average length of the plasma (L_p)

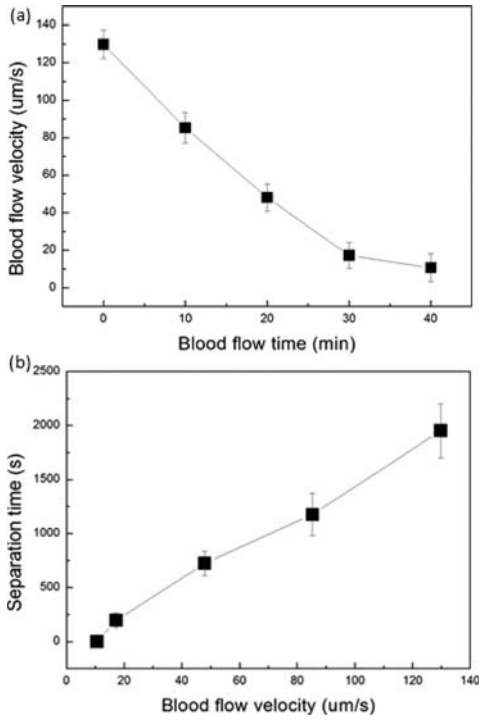

Fig. 7 (a) The relationship between the flow velocity of the whole blood samples in the channel and time. Under the influence of cell aggregation mass and capillary force, the blood flow velocity decreased as time passed. (b) The relationship between separation time and the initial whole blood flow velocity after the voltage was turned on at 1 Vp-p and 1 MHz. Each data point consists of at least three observations with one standard deviation as the error bar.

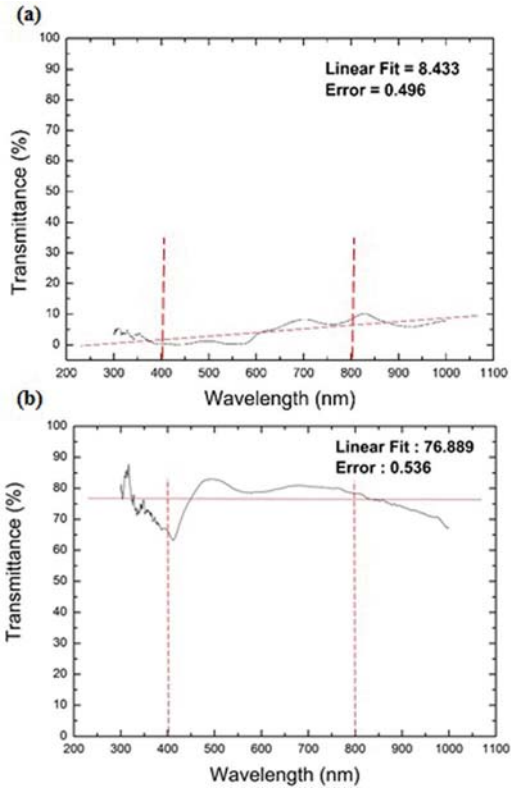

Fig. 8 The light transmittance of: (a) whole blood was 8.4% and (b) the separated plasma was 76.9% under the electric field and frequency applied of 1 V and 1 MHz, respectively. The measuring wavelengths were from 400 mn to 800 nm.

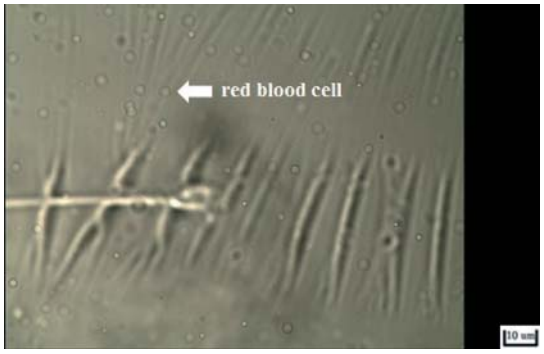

Fig. 9 There is minimal hemolysis noted in the separated plasma as the red blood cells are clearly seen in their perfect discoid shape under the image of an optical microscope.

was 67.65 mm. The volunteer's hematocrit was 41.8%, which was detected by the conventional method. Additionally, the separation quality was calculated using the modified Beer's Law, with the same experimental trials. The light transmittance was detected by the micro spectrometer system, which gave the average plasma percentage transmittance and average whole blood percentage transmittance as 76.9% and 8.4%, respectively, as shown in Fig. 8. The concentration of hemoglobin of the separated plasma, c, was calculated as 1.57 g dL^{-1}. The separation efficiency and separation quality in the experiments were 69.8% and 89.4%, respectively. Furthermore, minimal hemolysis was noted in the separated plasma (Fig. 9). The discoid shape of the red blood cell is intact and clearly seen.

Conclusion

An innovative, portable, disposable, capillary-driven and low-voltaged cDEP plasma separation chip has been proposed, fabricated and fully characterized in this work. The geometrically asymmetric capacitively-coupled electrodes induce the inhomogeneous electrostatic forces in the microchannel, which increased the dipole–dipole interactions between the red blood cells. Different frequencies and voltages were applied to study the separation times for the plasma. The effect of capillary force on plasma separation time and the velocity of the sample were also studied. This cDEP plasma separation chip has successfully separated the plasma from undiluted human whole blood samples without any external driven force. There were no visible bubbles produced, or high joule heat detected, and more importantly, no appearance of hemolysis noted. With such low-voltages applied, the biochip outputted a separation efficiency and a separation quality of 69.8% and 89.4%, respectively, within a reasonable separation time.

Notes and references

1 T. Kobayashi, T. Funamoto, M. Hosaka and S. Konishi, *Jpn. J. Appl. Phys.*, 2010, **49**, 077001–077005.
2 A. Oki, M. Takai, H. Ogawa, Y. Takamura, T. Fukasawa, J. Kikuchi, Y. Ito, T. Ichiki and Y. Horiike, *Jpn. J. Appl. Phys., Part 1*, 2003, **42**, 3722–3727.
3 X. Chen, D. F. Cui, C. C. Liu and H. Li, *Sens. Actuators, B*, 2008, **130**, 216–221.
4 M. Yamada and M. Seki, *Lab Chip*, 2005, **5**, 1233–1239.
5 S. S. Kuntaegowdanahalli, A. A. S. Bhagat, G. Kumar and I. Papautsky, *Lab Chip*, 2009, **9**, 2973–2980.
6 M. G. Lee, S. Choi, H. J. Kim, H. K. Lim, J. H. Kim, N. Huh and J. K. Park, *Appl. Phys. Lett.*, 2011, **98**, 2537021–2537023.
7 R. Fan, O. Vermesh, A. Srivastava, B. K. H. Yen, L. D. Qin, H. Ahmad, G. A. Kwong, C. C. Liu, J. Gould, L. Hood and J. R. Heath, *Nat. Biotechnol.*, 2008, **26**, 1373–1378.
8 Y. Fung, *Microvasc. Res.*, 1973, **5**, 34–48.
9 W. B. Betts and A. P. Brown, *J. Appl. Microbiol.*, 1999, **85**, 201S–213S.
10 R. Pethig, *Biomicrofluidics*, 2010, **4**, 022811.
11 H. A. Pohl and J. S. Crane, *Biophys. J.*, 1971, **11**, 711–727.
12 H. H. Cui, J. Voldman, X. F. He and K. M. Lim, *Lab Chip*, 2009, **9**, 2306–2312.
13 E. Du and S. Manoochehri, *Electrophoresis*, 2008, **29**, 5017–5025.
14 M. B. Sano, J. L. Caldwell and R. V. Davalos, *Biosens. Bioelectron.*, 2011, **30**, 13–20.
15 H. Shafiee, M. B. Sano, E. A. Henslee, J. L. Caldwell and R. V. Davalos, *Lab Chip*, 2010, **10**, 438–445.
16 W. M. Arnold and U. Zimmermann, *Z. Naturforsch., C: J. Biosci.*, 1982, **37**, 908–915.
17 H. Shafiee, J. L. Caldwell, M. B. Sano and R. V. Davalos, *Biomed. Microdevices*, 2009, **11**, 997–1006.
18 R. Pethig and D. B. Kell, *Phys. Med. Biol.*, 1987, **32**, 933–970.
19 A. Kumar, Z. Y. Qiu, A. Acrivos, B. Khusid and D. Jacqmin, *Phys. Rev. E: Stat., Nonlinear, Soft Matter Phys.*, 2004, **69**, 021402.
20 J. A. Wood and A. Docoslis, *J. Appl. Phys.*, 2012, **111**, 094106.
21 L. N. M. Duysens, *Biochim. Biophys. Acta*, 1956, **19**, 1–12.
22 C. K. Chung, H. C. Chang, T. R. Shih, S. L. Lin, E. J. Hsiao, Y. S. Chen, E. C. Chang, C. C. Chen and C. C. Lin, *Biomed. Microdevices*, 2010, **12**, 107–114.
23 C. K. Chung and S. L. Lin, *Int. J. Mach. Tool Manu.*, 2010, **50**, 961–968.